

# Characteristics of Seismic Activity in the Western, Central and Eastern Parts of the North Anatolian Fault Zone, Turkey: Temporal and Spatial Analysis

Serkan ÖZTÜRK

Gümüşhane University, Department of Geophysics, Gümüşhane, Turkey  
e-mail: serkanozturk@gumushane.edu.tr

## Abstract

Characteristics of seismic activity along the North Anatolian Fault Zone are analyzed between 1970 and 2010. Magnitude completeness changes between 2.7 and 2.9 in the North Anatolian Fault Zone. The frequency-magnitude distribution of earthquakes is well represented with a  $b$ -value typically close to 1. A clear decrease in temporal distribution of  $b$ -value is observed before the strong main shocks. Correlation dimension values are relatively large and the seismic activity is more clustered at larger scales in the North Anatolian Fault Zone.

A statistical assessment is made in order to detect the current seismic quiescence anomalies in the beginning of 2010. Eight significant anomalous zones throughout the North Anatolian Fault Zone are detected. These are centered at: (1) 41.08°N-28.58°E (around Silivri), (2) 41.47°N-29.51°E (in the Black Sea), (3) 40.69°N-29.78°E (including Izmit), (4) 40.26°N-26.46°E (around Gelibolu, Canakkale), (5) 40.59°N-31.03°E (including Duzce fault), (6) 40.86°N-35.30°E (around Amasya), (7) 39.48°N-39.74°E (around Erzincan), and (8) 39.06°N-40.50°E (around Bingol).

**Key words:** North Anatolian Fault Zone, seismic activity, fractal analysis, decluster, seismic quiescence.

## 1. INTRODUCTION

The space-time distribution of seismic activity and tectonics of the North Anatolian Fault Zone (NAFZ) in Turkey and different parts in the World have been investigated statistically and physically by many authors and some significant results have been obtained (e.g., Utsu 1971, Habermann 1983, Frohlich and Davis 1993, Wiemer and Wyss 2000, Ambraseys 2002, Huang *et al.* 2002, Yılmaz *et al.* 2004, Awad *et al.* 2005, Kutoglu and Akcin 2006, Kutoglu *et al.* 2008, Öztürk *et al.* 2008). The NAFZ is a major tectonic feature with a well-defined fault trace and an established history of seismicity. Because of topography and water resources, the fault zone is a relatively densely populated, agricultural area dotted by many villages and small towns. Most of the intermediate and large magnitude earthquakes occurring along the North Anatolian Fault (NAF) have produced surface breaks. Activity of the NAF during the 20th century began with the destructive Erzincan earthquake in 1939 in northeast Turkey and migrated westwards by a series of earthquakes in 1942, 1943, 1944, 1951, 1957, and 1967 (Toksöz *et al.* 1979, Barka 1996).

At the turn of the previous century, two destructive earthquakes occurred on the western continuation of the NAFZ in northwestern Turkey. The 17 August 1999,  $M_w$ 7.4, Izmit earthquake ruptured the NAFZ along a 145-km segment (Barka *et al.* 2002), which extended from Golyaka, Duzce, in the east, through the Izmit Bay into the Sea of Marmara in the west. The 12 November 1999,  $M_w$ 7.2, Duzce earthquake ruptured a segment about 41-km long, further to the east (Bürgmann *et al.* 2002). These two earthquakes are the latest in a sequence of large events that have ruptured an approximately 1000-km long section of the NAFZ.

In the present study, our main goal is to analyze the spatial and temporal properties of seismicity pattern in the North Anatolian Fault Zone in order to better understand the seismic hazards in this significant area. For this purpose, this study addressed the mapping of size-scaling distributions (e.g., spatial, temporal and magnitude distribution of seismic activity, completeness of magnitude,  $M_c$ , and  $b$ -values with time, seismic quiescence  $Z$ -value, fractal dimension,  $D_c$ ) in the regional scale, and the correlation of results with the structural elements which carry high risk for the region.

## 2. DATA AND TECTONICS OF THE NORTH ANATOLIAN FAULT ZONE

A part of the database used in this study is taken from Öztürk (2009). He developed some relationships between different magnitude scales (body wave magnitude,  $m_b$ , surface wave magnitude,  $M_s$ , local magnitude,  $M_L$ , duration magnitude,  $M_D$ ) in order to prepare a homogenous and complete earthquake

catalogue from different data sets. For this purpose, he used the catalogue data from the website of the International Seismological Centre (ISC) for the time period from 1970 to 1973 and Bogazici University, Kandilli Observatory and Research Institute (KOERI) for the time interval 1974 and 2005. Also different catalogues, such as National Telemetric Earthquake Observatory Network (TURKNET), Incorporated Research Institutions for Seismology (IRIS) and TÜBİTAK are used in order to obtain some unknown earthquakes. Öztürk (2009) prepared an instrumental data catalogue including  $M_D$  magnitude using these relationships. This catalogue for duration magnitude includes 73 530 earthquakes whose magnitudes are equal to or larger than 1.4, which occurred in Turkey between 1970 and 2005. For the period between 2006 and 2010, KOERI catalogue is also used. Seismological Observatory of KOERI, which has computed the size of all earthquakes with  $M_D$  (in general  $M_D > 3.0$ ), provides the real time data with the modern on-line and dial-up seismic stations in Turkey, especially after 2000. Thus, we used the  $M_D$  scale for more reliable results and we did not prefer to calculate new empirical values of different magnitude types. With regard to the accuracy of the seismic catalogue used in the present study, we can say that for earthquakes since the 1970s, errors in the epicenters are within 0-15 km and the errors in the magnitudes within 0.2, while the corresponding errors for the earthquakes prior to the 1970s are 0-30 km in epicenters and 0.5 in the magnitudes (Bogazici University home page, <http://www.boun.edu.tr/>).

Öztürk (2009) used the empirical relations in order to get a homogenous and complete catalogue from 1970 to 2005 and this smaller magnitude level  $M_D > 1.4$  is so obtained. In general, KOERI gives  $M_L$  magnitude for the local earthquakes with missing  $M_D$  magnitudes. In the situation that  $M_D$  is unknown in KOERI catalogue for the period between 2006 and 2010,  $M_D$  magnitudes are calculated using the relationships from Öztürk (2009) and 18 077 earthquakes are obtained for this time interval in and around Turkey.

The bounds of the region analyzed in this study are provided from Öztürk (2009). He divided Turkey into different 24 source regions considering the different previous zonation studies for seismic hazard modeling in Turkey, plotting the existing tectonic structure with the epicenter distribution of earthquakes, and solution of focal mechanism given by TÜBİTAK for the great earthquakes that occurred in Turkey between 1977 and 2002 (<http://www.mam.gov.tr/enstituler/ydbe/index.html>). Since Öztürk (2009) made a detailed zonation, part of these seismic source zones is considered as the study region. The North Anatolian Fault Zone (regions 20, 21 and 24 in Öztürk 2009) is selected as an area of investigation in this study. According to Öztürk (2009), region 20 (region 1 in this study) covers the Marmara part of the North Anatolian Fault Zone (MNAFZ), region 21 (region 2 in this study) is the Anatolian part of the North Anatolian Fault Zone (ANAFZ) and

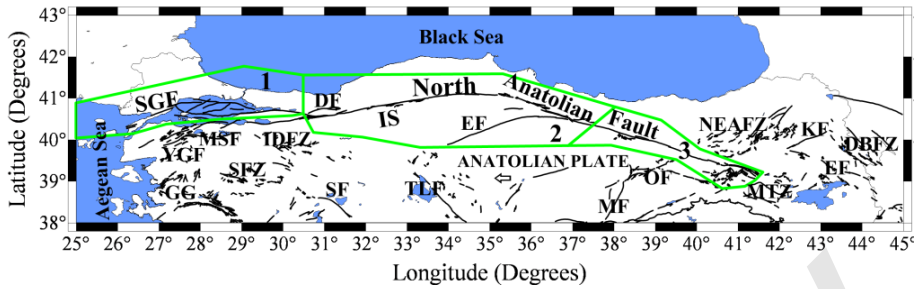


Fig. 1. Active tectonics and seismic source zones in the North Anatolian Fault Zone (NAFZ). Tectonic structures were modified from Şaroğlu *et al.* (1992) and the seismic regions from Öztürk (2009). Zones are marked: 1 – Marmara part of the NAFZ, 2 – Anatolian part of the NASF, 3 – Eastern part of the NAFZ. Names of faults: IS stands for Ismetpaşa segment, EF – Ercis Fault, DBFZ – Dogu Beyazit Fault Zone, NEAFZ – North East Anatolian Fault Zone, MTZ – Mus Thrust Fault Zone, KF – Kagızman Fault, SF – Sultandagı Fault, SFZ – Simav Fault Zone, SGF – Saros-Gazikoy Fault, IDFZ – Inonu-Dodurga Fault Zone, MF – Malatya Fault, YGF – Yenice-Gonen Fault, MSF – Manyas Fault, GG – Gediz Graben, DF – Duzce Fault, TLF – Tuz Lake Fault, OF – Ovacık Fault, EF – Ezinepazarı Fault. Colour version of this figure is available in electronic edition only.

region 24 (region 3 in this study) is the eastern part of the North Anatolian Fault Zone (ENAFZ). The major tectonic structures of the region adopted from Şaroğlu *et al.* (1992) and the zones from Öztürk (2009) are shown in Fig. 1 (One can find all details for the relationships of  $M_S$  magnitude and all seismic zonation in Bayrak *et al.* 2009).

After the selection of the study region as the North Anatolian Fault Zone, the earthquake data in this region is prepared. In this stage, the earthquakes between the time interval 2006 and 2010 for regions 1, 2, and 3 are selected from the whole catalogue. There are a total of 2804 events in these three regions between 2006 and 2010. The time interval considered for the present work is 1970 to 2010. The catalogue is homogeneous for duration magnitude and complete for whole study period and for all magnitude levels. Thus, the final data catalogue for region 1 (9884 events), region 2 (4669 events) and region 3 (2645 events) consists of 17 198 earthquakes in total (depth < 70 km) with magnitudes greater than or equal to 1.4. Epicenter distributions of whole earthquakes ( $M_D \geq 1.4$ ) and the principal main shocks ( $M_D \geq 5.5$ ) in the study region are shown in Fig. 2. All details of  $M_D \geq 5.5$  earthquakes are also given in Table 1.

The North Anatolian Fault is recognized as one of the most seismically active strike-slip faults in the World. This transform fault zone forms the part of the boundary between the Eurasian Plate to the north and Anatolian Plate to the south, being sub-parallel to the Black Sea coast. The NAFZ extends

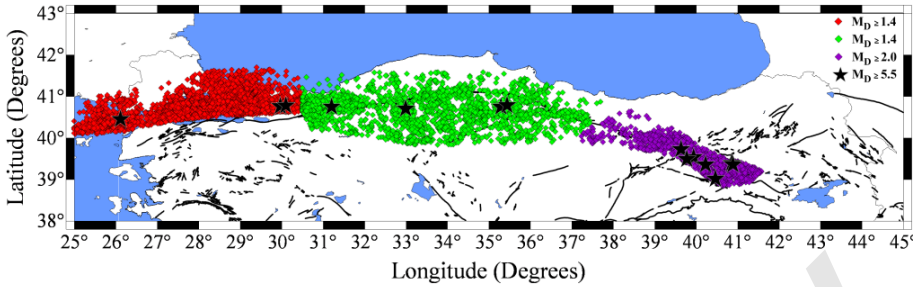


Fig. 2. Epicenter distributions of all earthquakes with  $M_D \geq 1.4$  and depth  $< 70$  km in the North Anatolian Fault Zone between February 1970 and December 2009. Stars represent the principal main shocks with  $M_D \geq 5.5$ . Colour version of this figure is available in electronic edition only.

Table 1

Some information of earthquakes occurred in study region with magnitude  $M_D \geq 5.5$

Date	Origin Time h m s	Longitude	Latitude	Depth [km]	$M_D$	Region	Location
27 Mar 1975	05 15 08	26.12	40.45	15.0	5.7	1	Gelibolu
13 Mar 1992	17 18 39	39.63	39.72	23.0	6.5	3	Erzincan
15 Mar 1992	16 16 25	39.93	39.53	29.0	6.0	3	Tunceli
05 Dec 1995	18 49 32	40.22	39.35	33.0	5.6	3	Tunceli
14 Aug 1996	01 55 03	35.29	40.74	17.0	5.6	2	Amasya
08 Mar 1997	23 01 58	35.44	40.78	5.0	6.0	2	Amasya
17 Aug 1999	00 01 37	29.97	40.76	18.0	6.7	1	Izmit
13 Sep 1999	11 55 28	30.10	40.77	19.0	5.8	1	Izmit
12 Nov 1999	16 57 21	31.21	40.74	25.0	6.5	2	Duzce
06 Jun 2000	02 41 49	32.99	40.70	5.0	5.6	2	Çankırı
27 Jan 2003	05 26 08	39.77	39.48	5.0	6.1	3	Tunceli
01 May 2003	00 27 04	40.46	39.01	5.0	6.2	3	Bingol
12 Mar 2005	07 36 09	40.85	39.39	4.0	5.6	3	Bingol
14 Mar 2005	01 55 55	40.88	39.35	5.0	5.9	3	Bingol

from the Gulf of Saros in the northern Aegean Sea to the town of Karliova in Eastern Turkey for 1200 km, paralleling roughly the southern Black Sea shores and keeping a fairly regular distance of some 100 km to the coast (Şengör *et al.* 2004). The dextral shear associated with the NAF continues across the northern Aegean, crosses northern and central mainland Greece as a broad shear and eventually links up with the Hellenic subduction zone. This fault zone is also characterized by several second order faults that splay from it into the Anatolian Plate (Bozkurt 2001). In general, while the fault exhibits strike-slip faulting with reverse component in the east owing to constricting of the Arabian plate, by converse, the western part shows normal

component due to interaction of the Aegean extensional regime. The NAFZ accommodates 24-30 mm/year of dextral motion (Reilinger *et al.* 1997). It has been estimated that its cumulative displacement of the fault varies from 40 km to a few hundred meters. The North Anatolian fault has experienced many damaging earthquakes during the past 60 years. The Karliova section has ruptured during two successive earthquakes on 19 and 20 August 1966,  $M6.8$  and  $M6.2$ , respectively (Ambraseys and Zátopek 1968, Ambraseys 1988a, b). The Erzincan earthquake of 26 December 1939 ( $M7.9$  to  $8.0$ ) is one of the greatest earthquakes that occurred in Turkey. This earthquake has played role as a trigger to the other earthquakes of the 1939-1967 sequences occurred in a westward progression: 20 December 1942 Erbaa-Niksar ( $M7.1$ ), 26 November 1943 Tosya ( $M7.6$ ), 1 February 1944 Bolu-Gerede ( $M7.3$ ), 13 August 1951 Çankırı ( $M6.9$ ), 26 May 1957 Abant ( $M7.0$ ), 22 July 1967 Mudurnu valley ( $M7.1$ ). The earthquakes that occurred in recent years in the NAFZ are: 13 March 1992 Erzincan ( $M6.8$ ), 17 August 1999 Izmit ( $M7.4$ ), and 12 November 1999 Duzce ( $M7.2$ ) earthquake, respectively (Bozkurt 2001).

### 3. BRIEF DESCRIPTION OF THE METHODS USED

The behavior of seismic activity analyzed in this study is restricted to shallow events ( $<70$  km). The 70 km maximum depth is adopted in this study since, in general, the seismogenic layer is suggested to be only 35-40 km thick for western Turkey (Özacar *et al.* 2009); however, on the basis of errors in hypocentral location, the less stringent lower limit of 70 km is adopted. In order to characterize the seismic behavior, a number of statistical parameters are used; namely size-scaling parameters (such as slope of recurrence curve  $b$ -value), temporal and spatial distribution of earthquakes with characteristics of fractal correlation dimension,  $D_c$ , and seismic quiescence  $Z$ -value as well as the histograms of temporal, spatial and magnitude distribution along the North Anatolian Fault Zone.

#### Seismic $b$ -value (magnitude-frequency relation) and completeness magnitude, $M_c$

The frequency-magnitude distribution (Gutenberg and Richter 1944) describing the relation between the frequency of occurrence and magnitude of earthquakes can be given as

$$\log_{10} N(M) = a - bM, \quad (1)$$

where  $N(M)$  is the expected number of events which occur during a given time period in relation to their magnitudes,  $M$ . The parameters  $a$  and  $b$  are constants. The  $a$ -value shows the activity level of seismicity. The  $b$ -value is the slope of the frequency-magnitude distribution. The  $a$  and  $b$ -values are

calculated empirically from seismic catalogues. The parameter  $a$  exhibits significant variations from region to region as it depends on the period of observation and the length of the considered area as well as the size of earthquakes. However, estimates of  $b$ -value imply a fractal relation between frequency of occurrence and the radiated energy, seismic moment, or fault length, and this is one of the most widely used statistical parameters to describe the size scaling properties of seismicity. Utsu (1971) summarized that  $b$ -values change roughly in the range from 0.5 to 1.5, depending on the different region. However, on average, the regional scale estimates of  $b$ -value are approximately equal to 1 (Frohlich and Davis 1993). The  $b$ -value can be estimated from the maximum likelihood method (Aki 1965)

$$b = 2.303 / (M_{\text{mean}} - M_{\text{min}} + 0.05) , \quad (2)$$

where  $M_{\text{mean}}$  and  $M_{\text{min}}$  are the mean magnitude of events and the minimum magnitude of completeness in the earthquake catalogue, respectively. The value 0.05 in eq. (2) is a correction constant. The 95% confidence limits on the estimates of  $b$ -value are  $\pm 1.96 b / \sqrt{n}$ , where  $n$  is the number of earthquakes used to make the estimate.

The minimum magnitude of complete recording,  $M_c$ , is an important parameter for many studies related to seismicity. In seismicity studies, it is frequently necessary to use the maximum number of events available for high-quality results. Estimating of  $M_c$  can be made by the assumption of Gutenberg–Richter's power-law distribution against magnitude (Wiemer and Wyss 2000). In order to investigate the seismic quiescence and the frequency-magnitude relationship, the change of  $M_c$  as a function of time is determined using a moving window approach with maximum likelihood method. Magnitude completeness in the catalogues varies systematically as a function of space and time, and the temporal variations can potentially result in a wrong value of seismicity parameters, especially in  $b$ -value. Because the network may be improved after the main shock and during the first highest activity, small shocks may not be located since they fall within the coda of larger events; and  $M_c$  will be higher in the early part of the earthquake catalogue (Wiemer and Katsumata 1999). Since part of this study deals with the seismicity rate change and not of energy or moment release, the magnitude of completeness of the catalogue used to detect the quiescence is an important parameter because this changes regionally, depending on the seismic activity of the area under investigation and the detectability of the network.

### **Fractal dimension, $D_c$**

Earthquake distributions are considered fractal, but indirectly. Fractal distributions imply that the number of objects larger than a specified size has

a power law dependence on the size. The fractal distributions are the only distributions that do not include a characteristic length scale, and therefore, are applicable to scale invariant phenomena. Spatial patterns of earthquake distribution and temporal patterns of occurrence are demonstrated to be fractal using the two-point correlation dimension,  $D_c$ . The correlation dimension measures the spacing or clustering properties of a set of points. The correlation integral method was developed by Grassberger and Procaccia (1983) and correlation dimension,  $D_c$ , is obtained from the following equations:

$$D_c = \lim_{r \rightarrow 0} [\log C(r) / \log r] , \quad (3)$$

$$C(r) = 2N_{R < r} / N(N-1) , \quad (4)$$

where  $C(r)$  is the correlation function,  $r$  is the distance between two epicenters or hypocenters, and  $N$  is the number of events pairs separated by a distance  $R < r$ . Fractal dimension is defined by fitting a straight line to a plot of  $\log C(r)$  against  $\log r$ . Here  $r$  refers to the distance between each two hypocenters as stated in Awad *et al.* (2005) and Polat *et al.* (2008).

The nature of temporal-spatial fractal properties of the earthquake epicenters is characterized by fractal, in particular by the correlation dimension (Kagan 2007). Fractal dimension,  $D_c$ , can be calculated to avoid the possible unbroken sites, and these unbroken sites have been suggested as potential *seismic gaps* to be broken in the future and  $D_c$  is related to hypocentral distance and to the physical models based on fluctuations in the elastic interactions between individual earthquake events (Toksöz *et al.* 1979). For the hypocenter distribution (3D space), the uniform distribution is in accordance with eq. (4) and it decreases with an increase in the clustering of events (Awad *et al.* 2005). It is reasonable to assume that the higher  $D_c$  and lower  $b$ -values are the dominant structural feature in the study area and may arise due to clusters. It is also an indication of changes in stress (Polat *et al.* 2008).

### **Declustering of the catalogues and seismic quiescence Z-value**

Aftershock activity generally masks temporal variations of the earthquake numbers and the related statistics. For the quantitative analysis of seismicity rate changes, it is necessary to eliminate the dependent events from the catalogue. To separate the dependent events from the independent ones, the earthquake catalogue is declustered using the Reasenberg (1985) algorithm. The cluster analysis algorithm of Reasenberg (1985) “declusters” or decomposes a regional earthquake catalogue into main and secondary events. It removes all the dependent events from each cluster, and substitutes them with a unique event, equivalent in energy to that of the whole cluster. The



ZMAP software in Wiemer (2001) is used for the declustering method based on the algorithm developed by Reasenber (1985). Only the epicenter and depth error values are changed. Other standard parameters are defined as given in the software.

In region 1, there are 9884 events with magnitudes greater than or equal to 1.4. The completeness magnitude,  $M_c$ , for region 1 is 2.7 and the number of earthquakes exceeding this magnitude threshold is 6514. The declustering procedure took away 258 (about 4%) events and 37% of the events in total were removed from the whole catalogue of region 1. Thus, the number of events for Z-value analysis was reduced to 6256 for the Marmara part of the North Anatolian Fault Zone. There are 4669 events in region 2 with magnitudes greater than or equal to 1.4. The  $M_c$  value for this region is 2.9 and the number of earthquakes exceeding this magnitude threshold is 3224. The declustering algorithm took away 267 (about 8%) events and 37% of the events were totally removed from whole catalogue of region 2. As a result, the number of events for Z-value analysis was reduced to 2947 for the Anatolian part of the North Anatolian Fault Zone. In region 3, there are 2645 earthquakes with magnitudes greater than or equal to 2.0. The  $M_c$  value for region 3 is 2.9 and the number of earthquakes exceeding this magnitude threshold is 1980. The declustering process took away 417 (about 21%) events and thus 41% of the events were totally removed from whole catalogue of region 3. Consequently, the number of events for Z-value analysis was reduced to 1563 for the eastern part of the North Anatolian Fault Zone and after completing the declustering processes, a more reliable, homogeneous and robust seismicity data has been obtained.

The standard normal deviate Z-test is one of the statistical methods frequently used for analyzing seismic quiescence. A continuous image of space and time rate changes in seismicity is produced by ZMAP, creating a grid of geographical co-ordinates, and associating to each grid node a selected number of nearest events. The ZMAP method is applied for imaging the areas exhibiting a seismic quiescence. In order to rank the significance of quiescence, the standard deviate Z-test is used (Habermann 1983, Wiemer and Wyss 1994), generating the Log Term Average (LTA) function for the statistical evaluation of the confidence level in units of standard deviations

$$Z = (R_1 - R_2) / (S_1^2 / N_1 + S_2^2 / N_2)^{1/2} , \quad (5)$$

where  $R_2$  is the mean seismicity rate in the foreground window,  $R_1$  is the average number of events in the whole background period,  $S$  and  $N$  are the standard deviations and the number of samples, within and outside the window. The Z-value computed as a function of time, letting the foreground window slide along the time duration of catalogue, is called LTA.

#### 4. RESULTS OF SEISMICITY ANALYSIS AND DISCUSSION

A detailed investigation of the seismicity behavior in the North Anatolian Fault Zone is made by using the Gutenberg–Richter  $b$ -value, seismic activity rate changes,  $Z$ -value, fractal correlation dimension  $D_c$ -value and also by evaluating the histograms of the temporal, spatial and magnitude distribution in time intervals between 1970 and 2010. The Gutenberg–Richter  $b$ -value is the slope of the frequency-magnitude distribution and provides a relative measure of the likelihood of large and small magnitude seismicity in the region. The correlation between seismicity and the fractal properties of epicenter distribution characterize complex properties and patterns of earthquake seismicity. Fractal analysis undertakes direct comparison of seismicity and maximum magnitude variation. As a result, this study is focused on the correlation of seismicity  $b$ -value, seismic quiescence  $Z$ -value, fractal dimension,  $D_c$ , and interrelationships between some other seismicity parameters.

The cumulative number of earthquakes *versus* time in the three regions for original catalogue and for declustered events is shown in Fig. 3. As shown in Fig. 3a, there is no significant change of reporting as a function of time between 1970 and 1975 for region 1. There is a little change in the seismic activity after 1970 until 1997 for region 2 (Fig. 3b) while important change in the seismic activity for region 3 is observed after 2003 (Fig. 3c). But further on, great seismic changes are seen in these areas, especially after 2000. Also, time histograms for region 1 (Fig. 4a) and region 2 (Fig. 4b) between 1970 and 2010 indicate an increase in the number of recorded events in the year of 2000. However, the maximum increase in the number of earthquakes for region 3 (Fig. 4c) is observed in the year of 2003. Because many stations have been constructed in these regions in recent years, especially after 1999 great earthquakes in Izmit and Duzce, the other observatories and mainly KOERI provides the real time data with the modern on-line and dial-up seismic stations in Turkey. Consequently, the further improvement of the catalogue since then could probably be associated with man-made effects, tectonic stress changes in the region or changing of used software during the computation of magnitude.

In this study, many statistical assessment techniques of ZMAP software package have also been carried out (Wiemer 2001) on the three data sets of seismicity catalogues of the NAFZ. The earthquake magnitude in these three catalogues ranges from 1.4 to 6.7 with an exponential decay in their numbers from the lower to higher magnitudes. Figure 5 defines the histograms of magnitude distribution for the data sets of three regions. Most of the earthquakes are between 2.5 and 3.5, and a maximum  $M_D 2.7$  is observed for region 1 (Fig. 5a), and a maximum  $M_D 2.9$  for region 2 (Fig. 5b) and region 3 (Fig. 5c).

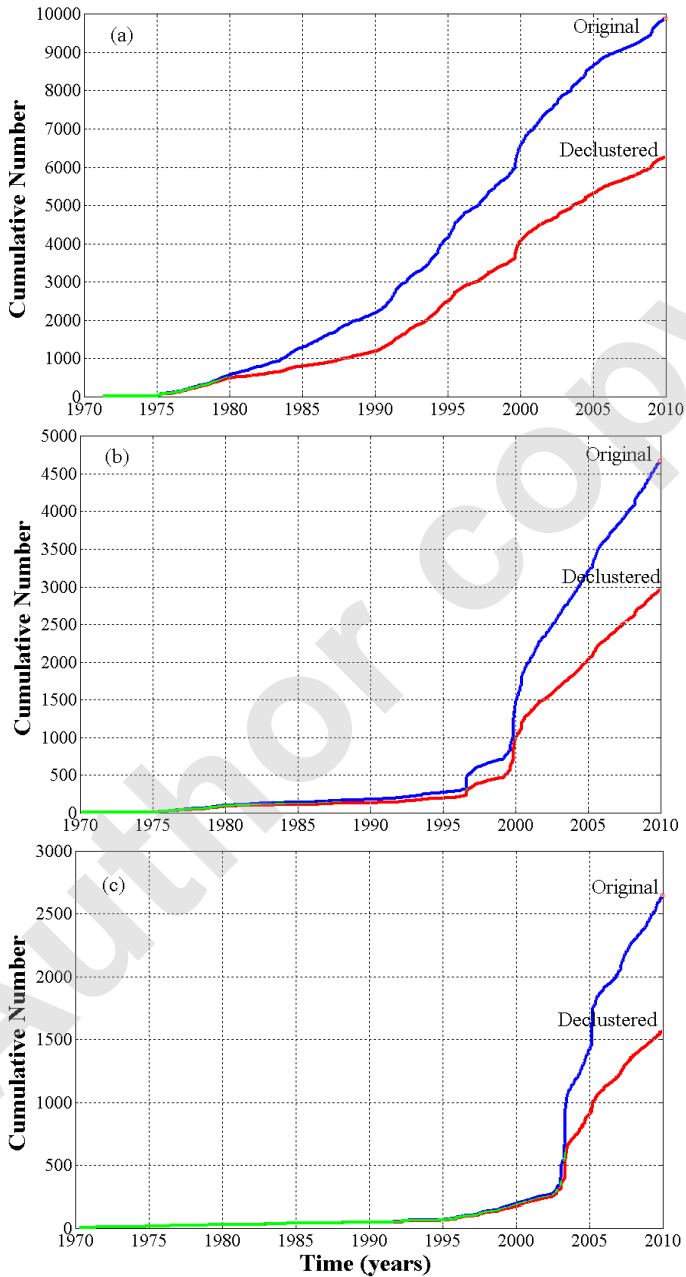


Fig. 3. Cumulative number of events against time for the original and declustered earthquake catalogue for: (a) region 1, Marmara part of the NAFZ, (b) region 2, Anatolian part of the NAFZ, and (c) region 3, eastern part of the NAFZ. Colour version of this figure is available in electronic edition only.

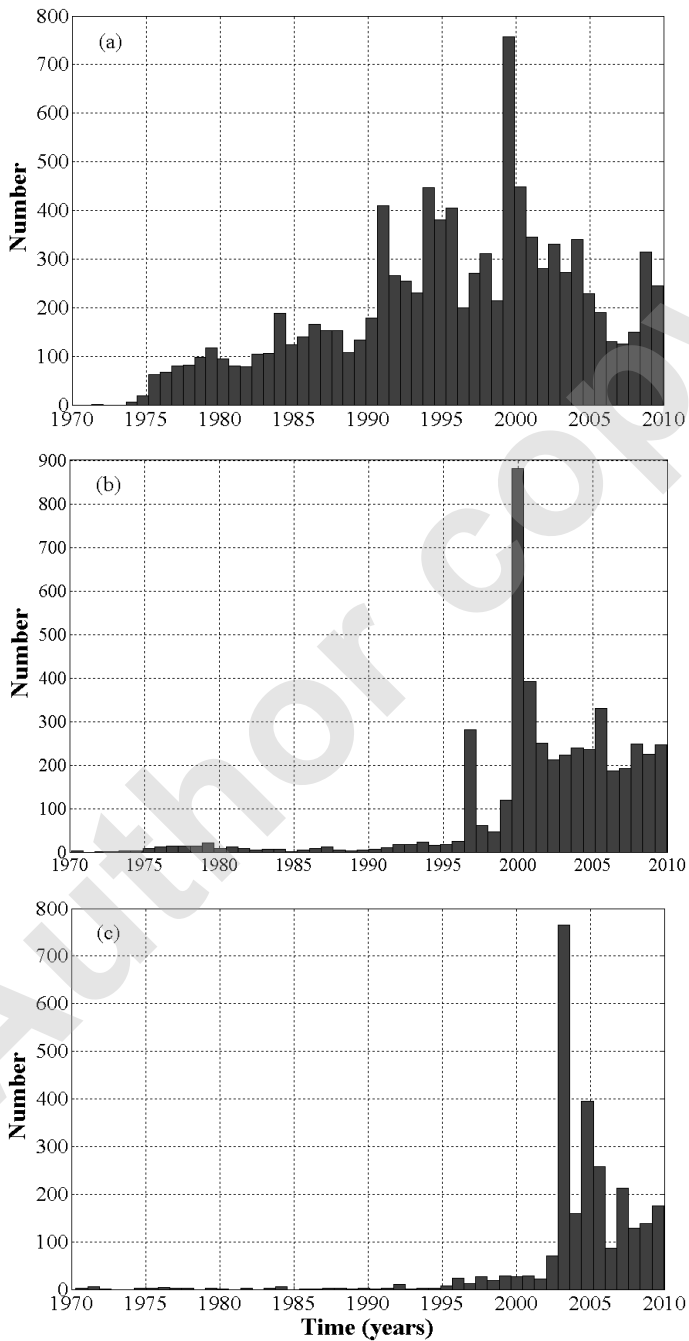


Fig. 4. Time histograms of the seismicity for data set of: (a) region 1, (b) region 2, and (c) region 3.

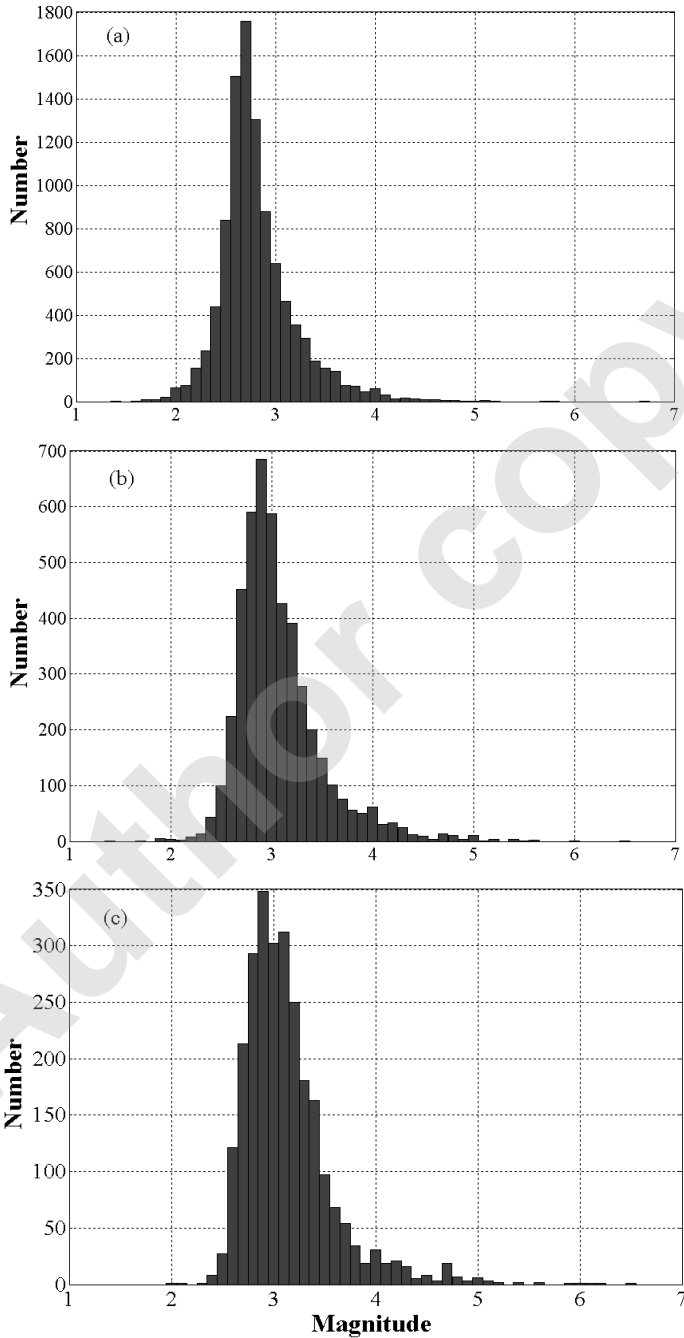


Fig. 5. Magnitude histograms of the seismicity for data set of: (a) region 1, (b) region 2, and (c) region 3.

In order to investigate the seismic quiescence and the frequency-magnitude relationship, the change of  $M_c$  as a function of time is determined using a moving window approach.  $M_c$  is estimated for samples of 30 events per window for region 1 by using the earthquake catalogue containing all 9884 events of  $M_D \geq 1.4$ , 75 events per window for region 2 by using the earthquake catalogue containing all 4669 events of  $M_D \geq 1.4$ , and 30 events per window for region 3 by using the earthquake catalogue containing all 2645 events of  $M_D \geq 2.0$ . Figure 6 shows the variations of  $M_c$  with time for all parts of the NAFZ. For region 1,  $M_c$  value is rather large and varies from 3.5 to 4.0 between 1975 and 1980 while  $M_c$  decreases to about 2.3 and 2.5 between 1980 and 1985 (Fig. 6a). Then, it decreases to about 2.7 in the beginning of 1987. However, there are two great values about 4.0 and 3.3. These large values in region 1 are observed after the 1999 Izmit earthquake sequence. For region 2,  $M_c$  has a value between 3.0 and 3.5 until 1985, and around 3.0 between 1985 and 2000 (Fig. 6b). This  $M_c$  value is smaller than 3.0 after 2000 and observed around 2.9. A large  $M_c$  value about 3.9 is observed in 1999 Duzce aftershock sequence. In these two parts of the NAFZ, as stated in Wiemer and Katsumata (1999), some high  $M_c$  values may be higher in the early part of the aftershock sequence because the small shocks may not be located. For region 3,  $M_c$  value is rather large and greater than 4.0 until 1995 and it decreases from 4.0 to 3.1 between 1995 and 2003 (Fig. 6c). After 2003,  $M_c$  value varies between 2.8 and 3.1. Therefore, it can be said that  $M_c$  generally shows a non-stable value in the different parts of the NAFZ. However, it can be easily said that  $M_c$  value varies between 2.7 and 2.9 in the NAFZ, and this result is consistent with the completeness analysis made by Huang *et al.* (2002).

Using ZMAP software, the  $b$ -value in Gutenberg–Richter (1944) relationship is calculated by the maximum likelihood method, because it yields a more robust estimate than the least-square regression method (Aki 1965). Gutenberg–Richter (G–R) law describes the statistical behavior of seismic zones in energy domain using the frequency magnitude of earthquakes (Awad *et al.* 2005). Figure 7 shows the plots of cumulative number of the earthquakes against the magnitude for all parts of the NAFZ. For the Marmara part of the North Anatolian Fault Zone (region 1), the whole catalogue includes 9884 earthquakes ( $M_D \geq 1.4$ ) for epicentral depths less than 70 km. The  $M_c$  value is calculated as 2.7 and using this value the  $b$ -value is calculated as  $1.13 \pm 0.01$  for region 1 (Fig. 7a). For the Anatolian part of the North Anatolian Fault Zone (region 2), the whole catalogue contains 4669 events ( $M_D \geq 1.4$ ) for epicentral depths less than 70 km. The completeness magnitude is computed as 2.9 and using this value of completeness the  $b$ -value is found as  $1.02 \pm 0.02$  for region 2 (Fig. 7b). For the eastern part of the North Anatolian Fault Zone (region 3), the whole catalogue includes 2645 events

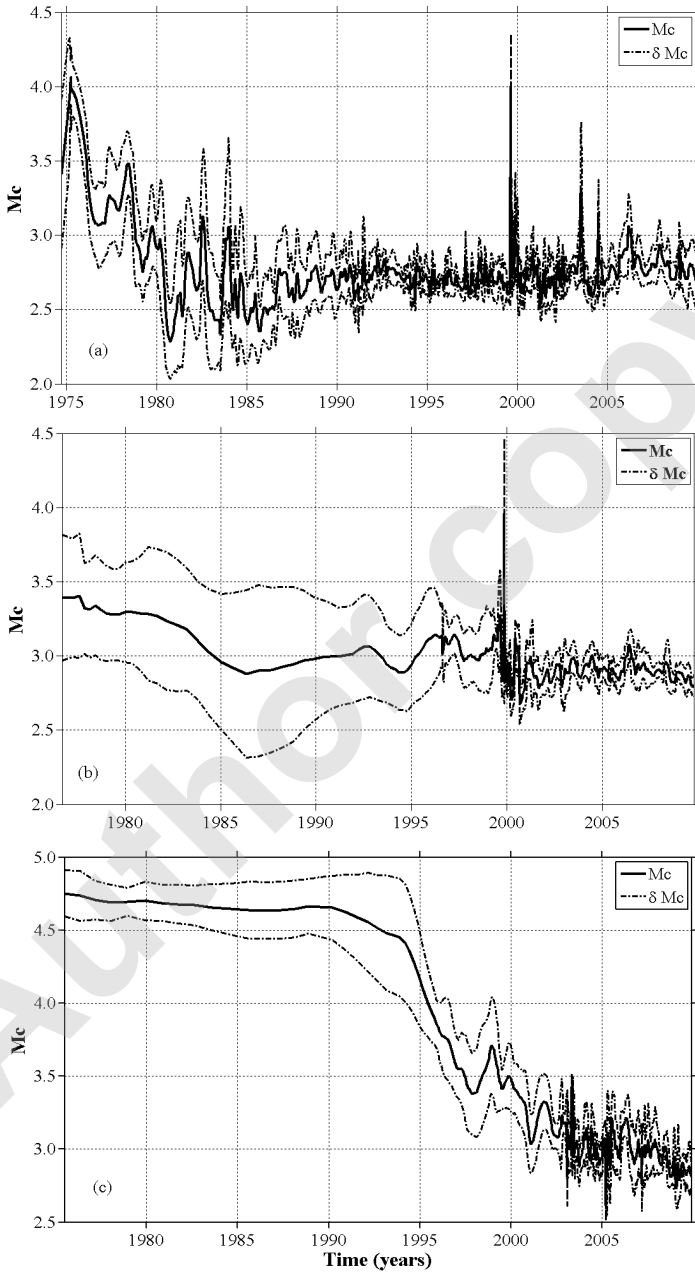


Fig. 6. Completeness magnitude,  $M_c$ , as a function of time for: (a) region 1, (b) region 2, and (c) region 3. Standard deviation,  $\delta M_c$ , of the completeness (dashed lines) is also given.  $M_c$  is computed for overlapping samples, each containing 30 events for region 1, 75 events for region 2, and 30 events for region 3, respectively.

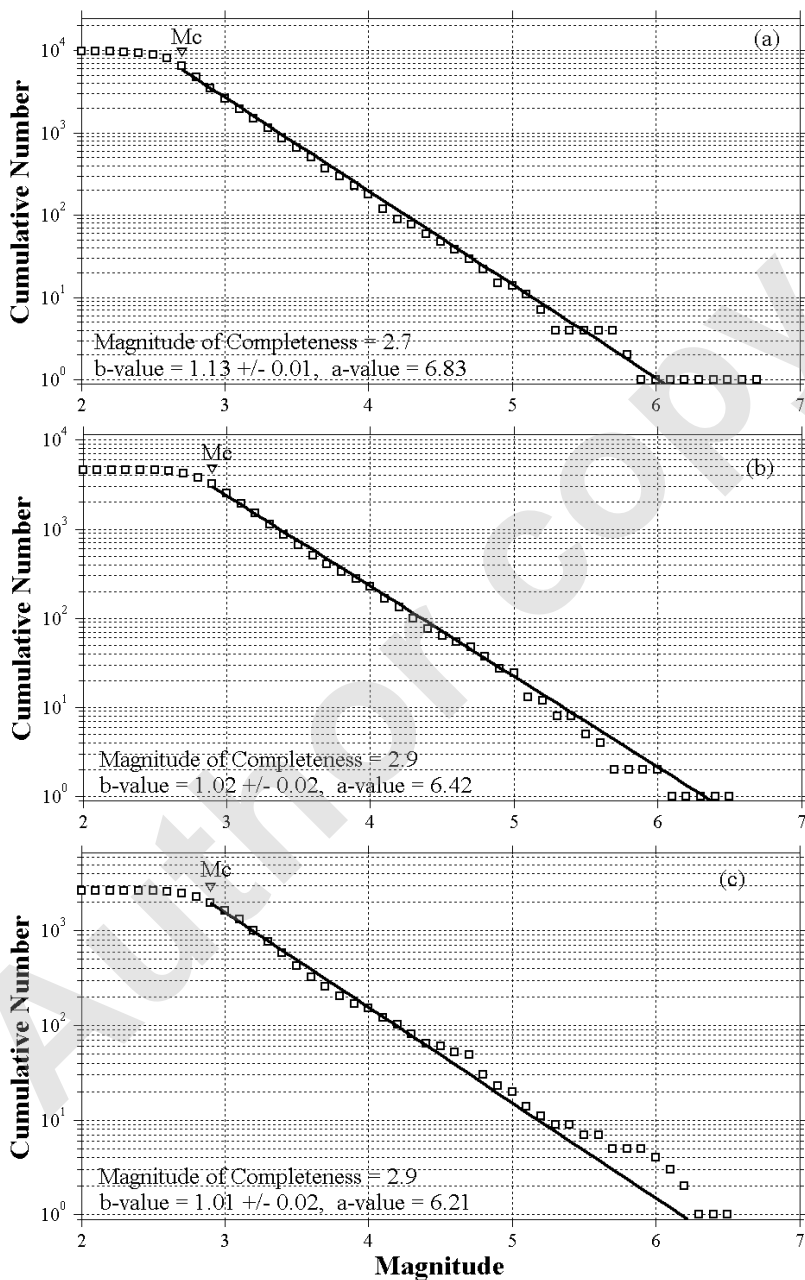


Fig. 7. Gutenberg–Richter relations and frequency–magnitude distributions of all earthquakes between 1970 and 2010 for: (a) region 1, (b) region 2, and (c) region 3. The  $b$ -value and its standard deviation, as well as the  $a$ -value in the Gutenberg–Richter relation are given.



( $M_D \geq 2.0$ ) for epicentral depths less than 70 km. The completeness magnitude,  $M_c$ , is taken as 2.9 and using this completeness value the  $b$ -value is computed as  $1.01 \pm 0.02$  for region 3 (Fig. 7c). For all regions, the  $b$ -value and its standard deviation is determined with the maximum likelihood method, as well as the  $a$ -value of Gutenberg–Richter relation. The tectonic earthquakes are characterized by the  $b$ -value from 0.5 to 1.5 and are more frequently around 1. It is clearly seen that the earthquake catalogue matches the general property of events such that magnitude-frequency distribution of the earthquakes is well represented by the Gutenberg–Richter law with a  $b$ -value typically close to 1.

The variation of the  $b$ -value as a function of time for different parts of the NAFZ is also analyzed (see Fig. 8). Temporal changes of  $b$ -value are calculated for sample size of 1000 earthquakes for region 1, and 250 earthquakes for regions 2 and 3, respectively. A systematic increase in  $b$ -value can be observed until 1996 with  $b > 1.5$  in region 1. The  $b$ -value shows a great decrease with  $b \approx 0.9$  before the occurrence of 1999 Izmit earthquake and a clear increase after the main shock (Fig. 8a). Such a kind of behavior is also observed for some strong earthquakes in regions 2 and 3. In region 2, there is a clear tendency of decrease with  $b \approx 0.7$  before the 1999 Duzce earthquake and an increase with  $b > 1.0$  after the main shock (Fig. 8b). In region 3, the same properties of  $b$ -value showing a decrease are observed before the three strong earthquakes. The  $b$ -values show a decrease before the occurrence of 2003 Tunceli, 2003 Bingol and 2005 Bingol earthquake sequences and a clear increase after the main shocks (Fig. 8c). Many factors can cause perturbations of the normal  $b$ -value. The  $b$ -value for a region does not reflect only the relative proportion of the number of large and small earthquakes in the region, but is also related to the stress condition over the region (Utsu 1971). Therefore, it is interpreted that the anomalies of decreases in  $b$ -value before the main shocks may be due to an increase in effective stress and can be used as an indicator of the future earthquake by observing the changes in  $b$ -value with time in all parts of the study region. Also, the stepwise increase in  $b$ -value is related to the reduced stress in these times after the main shocks.

The correlation dimensions for the distributions of earthquake hypocenters are obtained in different parts of the NAFZ. Correlation dimension,  $D_c$ , is estimated by fitting a straight (solid) line to the curve of mean correlation integral against the event distance,  $R$  (in km). The  $D_c$  values for all parts of the study area are obtained with 95% confidence limits by linear regression (Fig. 9). The earthquake distribution of 9884 earthquakes in the Marmara part of the North Anatolian Fault Zone is shown in Fig. 9a. The correlation dimension,  $D_c$ , is calculated as  $2.20 \pm 0.03$  for region 1. The earthquake distribution of 4669 events in the Anatolian part of the North Anatolian Fault

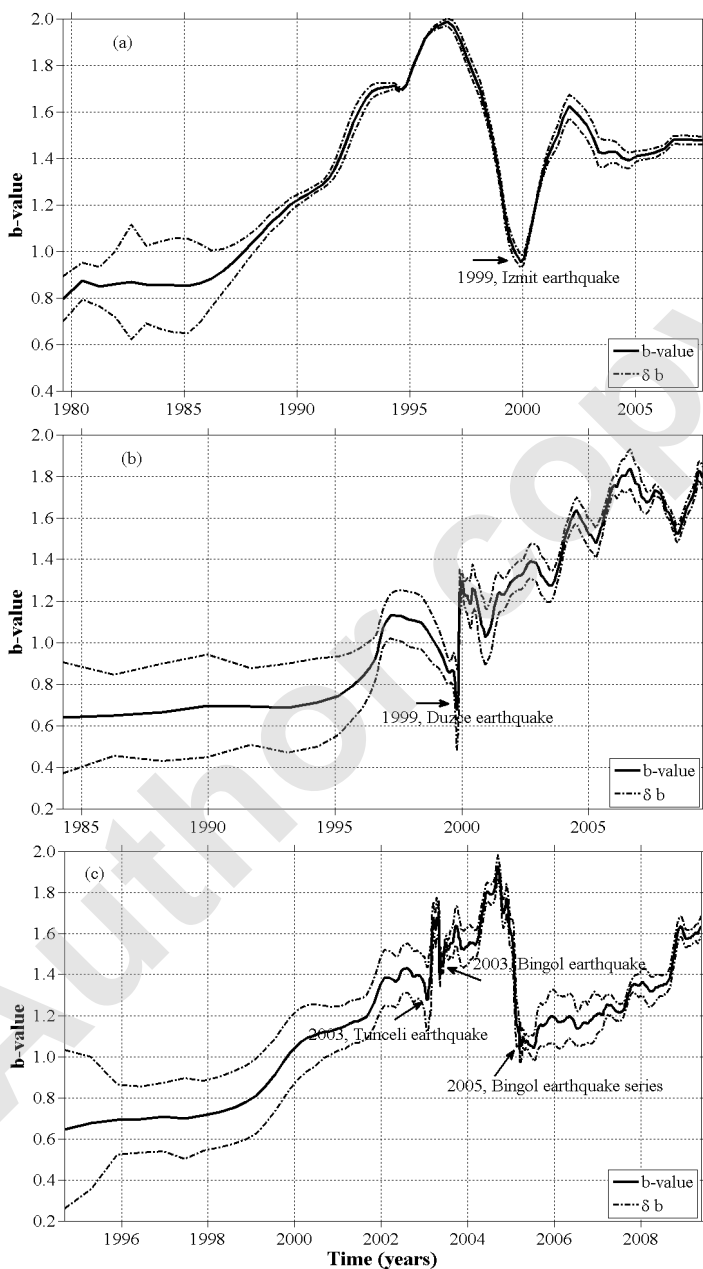


Fig. 8. The  $b$ -value as a function of time for: (a) region 1, (b) region 2, and (c) region 3. The  $b$ -values were computed for overlapping samples of 1000 earthquakes for region 1, 250 earthquakes for regions 2 and 3. Standard deviation,  $\delta b$ , of the  $b$ -values (dashed lines) is also given. Arrows show the great decrease in  $b$ -values before the large earthquakes in the regions.

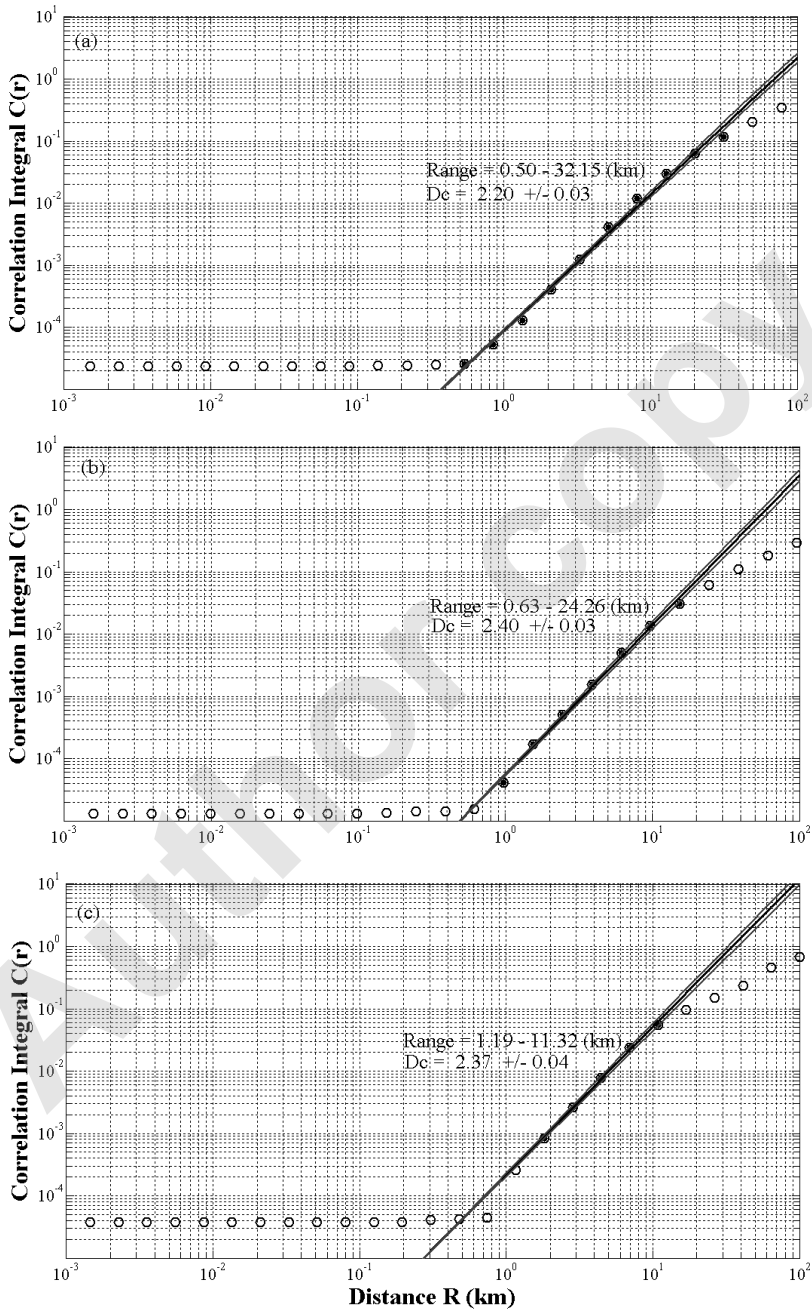


Fig. 9. Correlation integral curves *versus* distance for: (a) region 1, (b) region 2, and (c) region 3. Black dots represent the points in the scaling range. The slope of the black line corresponds to the  $D_c$  value and the gray lines illustrate the standard errors.

Zone is shown in Fig. 9b. The  $D_c$  is computed as  $2.40 \pm 0.03$  for region 2. The earthquake distribution of 2645 earthquakes in the eastern part of the North Anatolian Fault Zone is shown in Fig. 9c. The  $D_c$  is calculated as  $2.37 \pm 0.04$  for region 3. These log-log correlation functions exhibit a clear linear range and scale invariance in the cumulative statistics between 0.50 and 32.15 km for region 1 (indicated in Fig. 9a), between 0.63 and 24.26 km for region 2 (indicated in Fig. 9b) and, between 1.19 and 11.32 km for region 3 (indicated in Fig. 9c). The correlation dimension,  $D_c$ , and standard errors in Fig. 9 are also determined within these distances.

As earthquake distributions obey the fractal statistics, the fractal dimension can characterize them. Fractal properties of seismicity in the different regions of Turkey have been analyzed by using different catalogues and methods (Turcotte 1990). In the areas of increased complexity in the active fault system (higher  $D_c$ ) associated with lower  $b$ -value, the stress release occurs on fault planes of smaller surface area (Öncel and Wilson 2002). The higher order fractal dimension (greater than 2.20 for all regions) is increasingly sensitive to heterogeneity in the distribution of magnitudes. This suggests that seismicity is more clustered at larger scales (or in smaller areas) in the North Anatolian Fault Zone. Since the uniform distribution of earthquakes decreases with an increase in the clustering of events, it is reasonable to assume that the higher  $D_c$  values are the dominant structural feature in the study area and may arise due to clusters. Also, it can be an indication of changes in stress in the study region.

Spatial distribution of the standard deviate  $Z$ -value for all parts of the NAFZ is presented for the beginning of 2010 (Fig. 10). Each  $Z$ -value is displayed by different colors: the lowest  $Z$ -values are shown in blue and indicate that the change in seismicity rate is not significant, and the highest  $Z$ -values show a decrease in seismicity rate and are shown in red. Each  $Z$ -value in this representation is calculated in correspondence of a different grid point. The computed  $Z$ -values are then contoured and mapped. To establish a regional distribution of the seismic quiescence mentioned earlier, the Reasenber (1985) algorithm is applied to decluster the data. The areas under analysis were divided into rectangular cells spaced  $0.02^\circ$  in longitude and latitude. The nearest earthquakes,  $N$ , at each node are taken as 50 events after some preliminary tests for all regions and the seismicity rate changes are searched within the maximum radius changes by a moving time window,  $T_w$  (or  $iwl$ ), stepping forward through the time series by a sampling interval as described by Wiemer and Wyss (1994). The shape of the LTA function strongly depends on the choice of the length of the foreground window ( $iwl$ ). While the statistical robustness of the LTA function increases with the size of  $iwl$ , its shape becomes more and more smooth, if the  $iwl$  length exceeds the duration of the anomaly. The time window,  $T_w$ , equal to 5.5 years is used

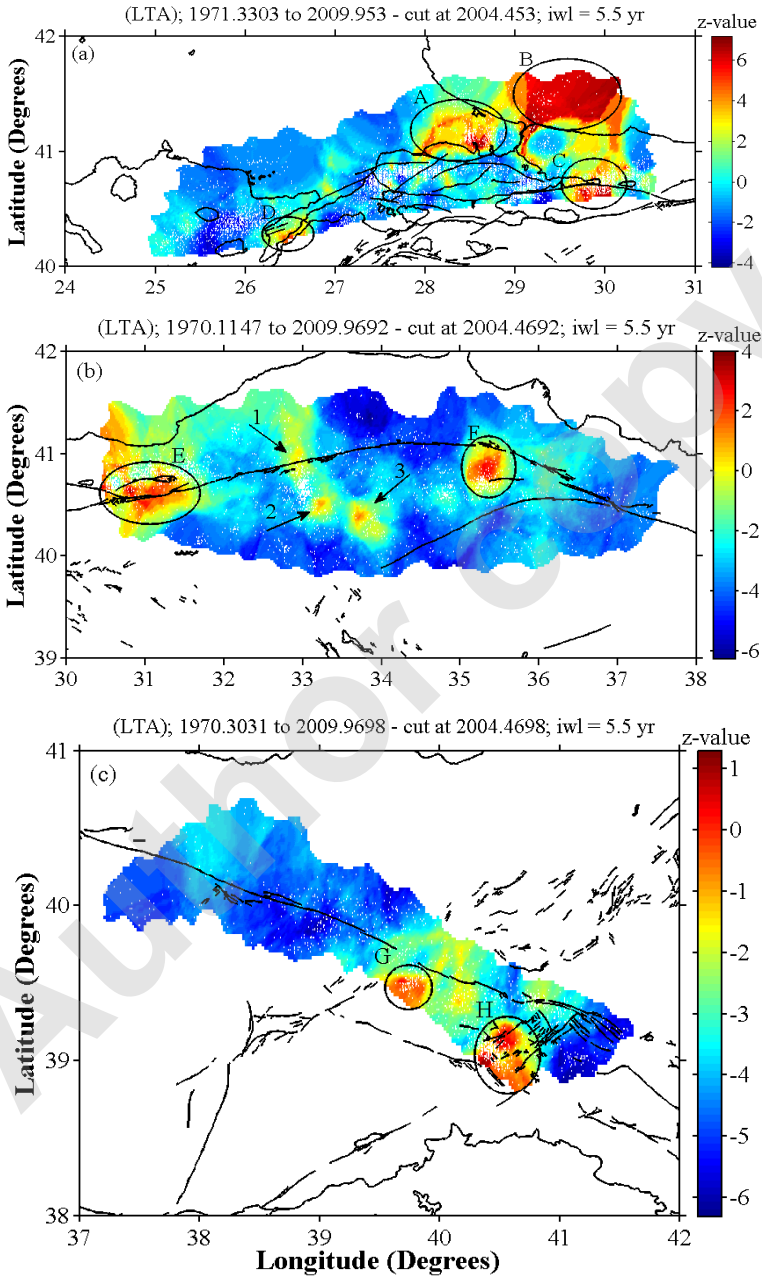


Fig. 10. Regional variability of Z-value in the beginning of 2010 with  $T_W(iwl)$  equal to 5.5 years for: (a) region 1, (b) region 2, and (c) region 3, respectively. White dots show the declustered earthquakes with  $M_D \geq 2.7$  for region 1,  $M_D \geq 2.9$  for regions 2 and 3. Colour version of this figure is available in electronic edition only.

as the window length because the quiescence areas are better visible for a window of 5.5 years. Since the quiescence anomalies found in Fig. 10 are the best revealed at the epicentral areas for  $T_W$  equal to 5.5 years it is used this time window length in order to image the geographical distribution of the seismicity rate changes. For each grid point we binned the earthquake population into many binning spans of 28 days for all regions in order to have a continuous and dense coverage in time. The  $N$  and  $T_W$  values are usually selected accordingly in order to enhance the quiescence signal and this choice does not influence the results in any way.

Figure 10a shows the geographical distribution of  $Z$ -values for region 1 including the Marmara part of the North Anatolian Fault Zone. As shown in Fig. 10a, four areas (A, B, C and D) exhibiting significant seismic quiescence are apparent. Figure 10b shows the spatial variations of  $Z$ -value for region 2 including the Anatolian part of the North Anatolian Fault Zone. As shown in Fig. 10b, there are two areas (E and F) exhibiting significant seismic quiescence. Figure 10c shows the regional distributions of  $Z$ -value for region 3 including the eastern part of the North Anatolian Fault Zone. As shown in Fig. 10c, two areas (G and H) exhibit significant seismic quiescence. In addition to these eight significant areas, there are some small quiescence areas in the Anatolian part of the North Anatolian Fault Zone. One of them is observed on Ismetpasa segment (arrow 1 in Fig. 10b) and the others on southwest (Çankırı) of this segment (arrows 2 and 3 in Fig. 10b). However, since these small quiescence areas are not very clear it is considered that they are not as significant as the other eight quiescence areas. Also, since there are fewer earthquakes in some edges (especially in Bleak Sea region, or the other regions that have no fault system), these values in the above-mentioned regions can be interpreted as artificial results from contouring and interpolations.

The length of time window for all figures is determined by adding  $T_W$  value in years to the time chosen as the beginning of the time cut (indicated in the corresponding figures). So, all figures show the  $Z$ -value distribution for the same time for all regions, in the beginning of 2010. Clear quiescence anomalies were identified at several seismogenic sources. In the  $Z$ -value maps for all parts of the North Anatolian Fault Zone, eight areas exhibit significant seismic quiescence. In region 1, covering the MNAFZ, the first significant anomaly is found centered at  $41.08^\circ\text{N}$ - $28.58^\circ\text{E}$  (region A, around Silivri) and the second one is found centered at  $41.47^\circ\text{N}$ - $29.51^\circ\text{E}$  (region B, in the Black Sea). The third significant quiescence is observed centered at  $40.69^\circ\text{N}$ - $29.78^\circ\text{E}$  (region C, including Izmit) and the fourth significant anomaly is found centered at  $40.26^\circ\text{N}$ - $26.46^\circ\text{E}$  (region D, around Gelibolu, Canakkale). In region 2, including the ANAFZ, the first significant anomaly is found centered at  $40.59^\circ\text{N}$ - $31.03^\circ\text{E}$  (region E, including Duzce fault) and

the second quiescence area is found centered at 40.86°N-35.30°E (region F, around Amasya). In region 3, covering the ENAFZ, the first significant anomaly is found centered at 39.48°N-39.74°E (region G, around Erzincan) and the second anomaly is found centered at 39.06°N-40.50°E (region H, around Bingöl).

In order to find all significant rate changes in the earthquake catalogues of the different parts on the NAFZ, computer code GENAS (Habermann 1983) is used. The GENAS calculates the cumulative numbers for different magnitude cutoffs. The purpose of separately investigating magnitude bins is to isolate the magnitude band in which individual reporting changes occur. Figure 11 shows the GENAS results searching for significant breaks in slope, starting from the end of data, and for all magnitude bins (**Mag and below** means all earthquakes with a magnitude smaller than  $M_D$ , while **Mag and above** means all earthquakes with a magnitude larger than  $M_D$ ). Figure 11a (region 1) shows a strong increase of reported small events in the 1975 and 1990. However, there are two strong decreases in 2005 and 2009 for small events. Also, some mild decreases of large events are noticeable in the 2005 and 2009 in region 1. Figure 11b shows GENAS results for region 2. A strong increase of reporting of small events is observed in 1975, 1992, 1996, and 2001. A strong decrease of small events and mild decrease of large events in 1980 is found. In addition, there are some mild decreases of large events between 2001 and 2009 in region 2. The GENAS results for region 3 are shown in Fig. 11c. There is a strong increase between 1992 and 1995 for small and large events. A strong change observed is an increase after 2003. Two strong decreases are observed in 2005 and 2008 for small events in region 3. Also, there is some little decrease of large events between 2005 and 2009. Thus, there is a clear consistence between the findings of seismic quiescence for the current time in Figs. 10 and 11.

In recent years, many studies have been made and different methods have been applied in order to present the spatial variability of earthquake hazard in several regions of Turkey, especially in the North Anatolian Fault Zone (e.g., Huang *et al.* 2002, Yılmaz *et al.* 2004, Kutoglu and Akcin 2006, Kutoglu *et al.* 2008, Öztürk *et al.* 2008).

Huang *et al.* (2002) made a study on the detection of seismic quiescence in and around the epicentral zone of the 17 August 1999,  $M_W$ 7.4, Izmit (Turkey) earthquake, by applying a statistical method, the Region-Time-Length (RTL) algorithm, to earthquake catalogues derived from that for the period 1981-1999 of KOERI, which are complete for events  $M_D \geq 3.0$  in most of western Turkey. The RTL parameter indicates that a period of seismic quiescence started at the end of 1995 and reached a minimum in December 1996. The main shock in Izmit and vicinity did not occur when the seismicity

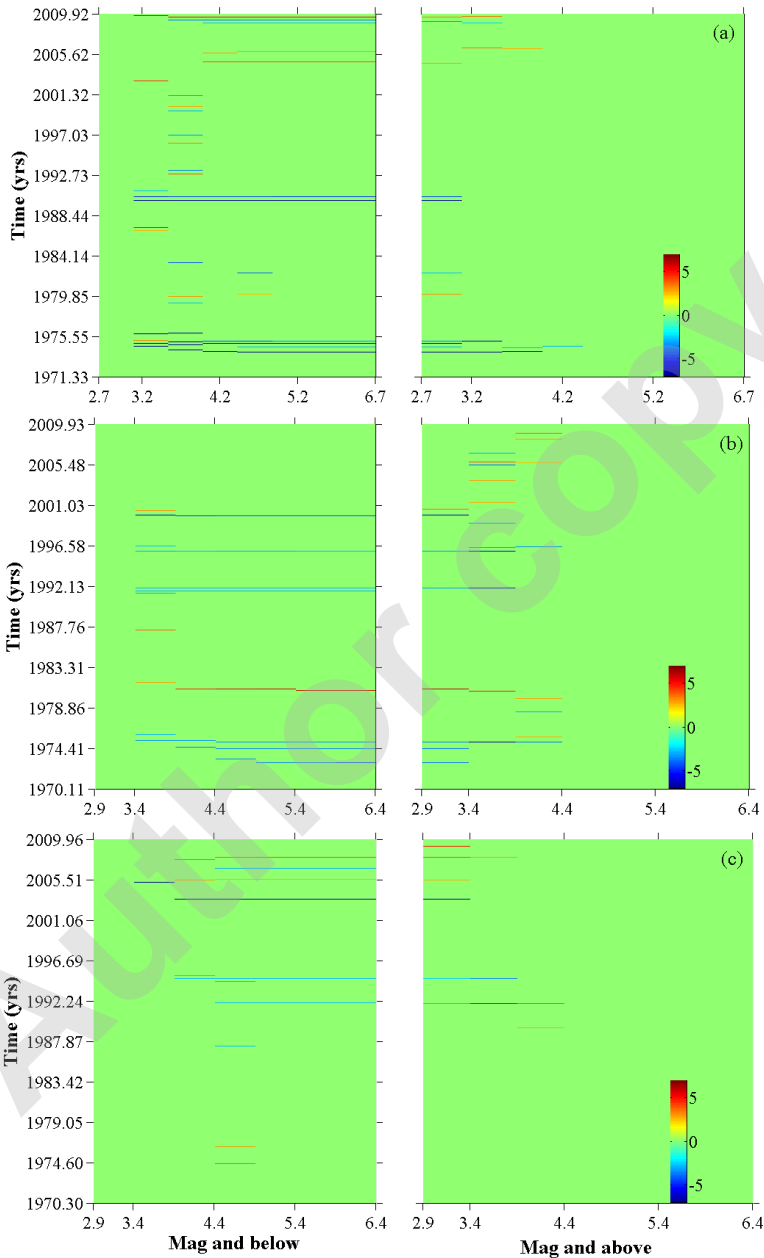


Fig. 11. The GENAS outputs for declustered data for: (a) region 1, (b) region 2, and (c) region 3. Times of significant rate changes as a function of time are shown. Times of significant changes (at the 99% confidence level) are marked in blue for seismicity rate increases and in red for seismicity rate decreases as a function of magnitude band. Colour version of this figure is available in electronic edition only.



returned to its background level, but occurred with a delay of nearly 2.5 years. Their results indicate that a significant quiescence anomaly appeared in 1996 around the epicenter of the Izmit earthquake. Similarly, in this study, some significant quiescence areas are observed in recent years in the Marmara part of the North Anatolian Fault zone including the Izmit main shock region. Thus, such kind of quiescence features could be recognized as a constant and reliable characteristic of seismicity, and they could eventually contribute to the forecast of impending main shocks in the future circumstances.

Yılmaz *et al.* (2004) used some statistical methods to characterize the seismic hazard or risk for different parts of the North Anatolian Fault Zone. They divided the NAFS into three areas (west, middle and east) in terms of different features such as the number of the earthquakes and magnitudes. They concluded that the risks of an earthquake occurrence with magnitude 5 or above in 5 years in the west, middle and east part of the North Anatolian Fault Zone are 84, 88, and 72%, respectively. The duration of significant anomalies in this study generally starts in the beginning of 2005 for all parts of the NAFZ. If it is considered the fact that the reported seismic quiescence prior to crustal main shocks varies from 1.5 to 5.5 years, it can be concluded that the regions where the significant quiescence anomalies are observed can be interpreted as the next earthquake areas with a mean probability greater than 70%.

Kutoglu and Akcin (2006) and Kutoglu *et al.* (2008) determined the surface creep on the Ismetpasa segment of the North Anatolian Fault Zone after the Izmit and Duzce earthquakes in 1999 that occurred in the near west of the Ismetpasa segment based on the periodical observations of an old trilateration network. Their evaluation of the observations revealed a creep of 0.78 cm/year for the period 1992-2002 and this new observation campaign of the Ismetpasa geodetic network shows that the Ismetpasa segment has ceased the slowing trend and started to gain speed. They interpreted that the Ismetpasa segment of the North Anatolian Fault Zone is under an increasing earthquake risk. Although the quiescence found in this study on the Ismetpasa segment (arrow 1 in Fig. 10b) is in a small region and is not very clear, this can be interpreted as an earthquake risk for this segment.

Öztürk *et al.* (2008) made a quantitative appraisal of earthquake hazard parameters using Gumbel's first asymptotic distribution for different regions in and around Turkey. They constructed a uniform catalogue of  $M_S$  in the period between 1900 and 2005. They estimated the mean return periods, the most probable magnitude and the probability of earthquake occurrence for a given magnitude in a period of 10, 25, 50, and 100 years for different 24 regions in and around Turkey. The results from Öztürk *et al.* (2008) show that the mean return period value for  $M_S \geq 5.5$  in their region 20 covering the

MNAFZ (region 1 in this study) is equal to  $11.22 \pm 0.39$  years. Also, the probability of occurrence for the earthquakes with this magnitude size in this region is equal to 60% in the next 10 years according to their study. The last event of magnitude  $M_D \geq 5.5$  occurred in 1999 (see Table 1) in region 1. So, the next time with a probability of 60% for that size of earthquakes can be considered as 2010 in the MNAFZ. For their region 21, including the ANAFZ (region 2 in this study), the value of the mean return period for  $M_S \geq 5.5$  is calculated as  $6.24 \pm 1.52$  years and the probability of occurrence for the earthquakes in this magnitude range is computed as 80% for the next 10 years by Öztürk *et al.* (2008). The last event of magnitude  $M_D \geq 5.5$  occurred in 2000 in region 2. The next time with a probability of 80% for that size of earthquakes can be considered as 2006 in the ANAFZ. Thus, the return periods have been exceeded for this size of main shocks. However, the mean return period for  $M_S \geq 6.0$  is found as  $11.48 \pm 1.59$  years in the ANAFZ by Öztürk *et al.* (2008). Also, the probability of occurrence for this magnitude size is computed as 58%. If this magnitude range is considered, the next time with a probability of 58% for  $M_D \geq 6.0$  can be considered as 2011 in the ANAFZ. In their region 24 related to the ENAFZ (region 3 in this study), the mean return period value for the earthquakes with  $M_S \geq 5.5$  is revealed by them with a value of  $7.50 \pm 0.09$  years and they computed the probability of occurrence for the earthquakes having the same size as 74% in the next 10 years. The last event of magnitude  $M_D \geq 5.5$  occurred in 2005 in region 3. So, the next time with a probability of 58% for that size of earthquakes can be considered as 2012 in the ENAFZ.

## 5. CONCLUSIONS

Spatial and temporal evaluations of the current seismic activity are carried out in order to characterize the seismic behavior in the different parts of the North Anatolian Fault Zone. For this purpose, a number of statistical parameters are used; namely size-scaling parameters (such as slope of recurrence curve  $b$ -value), seismic quiescence  $Z$ -value, temporal and spatial distribution of earthquakes with characteristic of fractal correlation dimension,  $D_c$ , as well as the histograms of temporal, spatial and magnitude distributions. For this purpose, statistical analysis techniques based on the seismic tool ZMAP are applied. The instrumental earthquake catalogues of KOERI, TURKNET, ISC, IRIS and TÜBİTAK between 1970 and 2010 are compiled and finally 17 198 crustal earthquakes of magnitude equal and greater than 1.4, with depths less than 70 km are obtained.

Seismicity characteristics in different parts of the NAFZ are nearly the same as an earthquake activity in all regions shows an important increase, especially after 2000. Magnitude completeness analyses present a value

between 2.7 and 2.9 for all parts of the NAFZ. The  $b$ -values for all regions are close to 1 and typical for earthquake catalogues. Temporal distributions of  $b$ -values show a strong tendency of decreasing before the large main shocks and this behavior can be used as an indicator of the next earthquake. Correlation dimension values are greater than 2.20 for all parts of the NAFZ. This suggests that seismic activity is more clustered at larger scales (or in smaller areas) in the NAFZ. Therefore, these higher values mean the dominant structural feature in the study area and may arise due to clusters.

In order to separate the dependent events, Reasenberg algorithm is used and the earthquake catalogues for all regions are declustered for the standard deviate  $Z$ -value calculations. The significance of seismicity rate changes is measured at the nodes of a  $0.02^\circ$  grid space in longitude and latitude for all parts of NAFZ. There are eight regions exhibiting significant seismic quiescence on the NAFZ in the beginning of 2010. On the Marmara part of the NAFZ, four anomalies are found centered at  $41.08^\circ\text{N}$ - $28.58^\circ\text{E}$  (around Silivri),  $41.47^\circ\text{N}$ - $29.51^\circ\text{E}$  (in the Black Sea),  $40.69^\circ\text{N}$ - $29.78^\circ\text{E}$  (including Izmit) and  $40.26^\circ\text{N}$ - $26.46^\circ\text{E}$  (around Gelibolu, Canakkale). The other two quiescence areas are found centered at  $40.59^\circ\text{N}$ - $31.03^\circ\text{E}$  (including Duzce fault) and  $40.86^\circ\text{N}$ - $35.30^\circ\text{E}$  (around Amasya) on the Anatolian part of the NAFZ. The rest of the quiescence anomalies are found centered at  $39.48^\circ\text{N}$ - $39.74^\circ\text{E}$  (around Erzincan) and  $39.06^\circ\text{N}$ - $40.50^\circ\text{E}$  (around Bingol) on the eastern part of the NAFZ. These areas of seismic quiescence recently observed, which started at the beginning of 2005 in eight aforementioned regions, can be considered as the most significant.

The NAFZ was struck with devastating earthquakes in recent years. Therefore, prediction of the future large earthquake in this area would be useful. Such an assessment must be relied on the observation of phenomena related to precursory quiescence. Previous studies for the NAFZ show that the return periods of  $M_D \geq 5.5$  have been exceeded in the Anatolian part of the NAFZ. However, the return periods of  $M_D \geq 5.5$  for the Marmara and the eastern part and the return period of  $M_D \geq 6.0$  for the Anatolian part of the NAFZ will be exceeded between 2010 and 2012. For this reason, special attention should be given to these regions where the seismic quiescence is observed and monitoring of their microseismic activity by locally dense arrays, as well as the monitoring of other geophysical parameters is suggested.

**Acknowledgements.** The authors would like to thank to Professor Stefan Wiemer for providing ZMAP software and three anonymous reviewers for their useful and constructive suggestions in improving this paper. We are grateful to Dr. Dogan Kalafat (KOERI) for providing us the earthquake catalogue. We also thank to Kandilli Observatory and Research Institute for providing earthquake database *via* Internet.

## References

- Aki, K. (1965), Maximum likelihood estimate of  $b$  in the formula  $\log N = a - bM$  and its confidence limits, *Bull. Earthq. Res. Inst. Tokyo Univ.* **43**, 237-239.
- Ambraseys, N.N. (1988a), Engineering seismology: Part I, *Earthq. Eng. Struct. Dyn.* **17**, 1, 1-50, DOI: 10.1002/eqe.4290170101.
- Ambraseys, N.N. (1988b), Engineering seismology: Part II, *Earthq. Eng. Struct. Dyn.* **17**, 1, 51-105, DOI: 10.1002/eqe.4290170102.
- Ambraseys, N.N. (2002), The seismic activity of the Marmara Sea Region over the last 2000 years, *Bull. Seism. Soc. Am.* **92**, 1, 1-18, DOI: 10.1785/0120000843.
- Ambraseys, N.N., and A. Zátópek (1968), The Varto Üstükran (Anatolia) earthquake of 19 August 1966 summary of a field report, *Bull. Seism. Soc. Am.* **58**, 1, 47-102.
- Awad, H., M. Mekkawi, G. Hassib, and M. Elbohoty (2005), Temporal and three dimensional spatial analysis of seismicity in the Lake Aswan area, Egypt, *Acta Geophys. Pol.* **53**, 2, 153-166.
- Barka, A. (1996), Slip distribution along the North Anatolian fault associated with the large earthquakes of the period 1939 to 1967, *Bull. Seism. Soc. Am.* **86**, 5, 1238-1254.
- Barka, A., H.S. Akyüz, E. Altunel, G. Sunal, Z. Çakır, A. Dikbaş, B. Yerli, R. Armijo, B. Meyer, J.B. de Chabaliér, T. Rockwell, J.R. Dolan, R. Hartleb, T. Dawson, S. Christofferson, A. Tucker, T. Fumal, R. Langridge, H. Stenner, W. Lettis, J. Bachhuber, and W. Page (2002), The surface rupture and slip distribution of the 17 August 1999 İzmit earthquake (M7.4), North Anatolian fault, *Bull. Seism. Soc. Am.* **92**, 1, 43-60, DOI: 10.1785/0120000841.
- Bayrak, Y., S. Öztürk, H. Çınar, D. Kalafat, T.M. Tsapanos, G.Ch. Koravos, and G.A. Leventakis (2009), Estimating earthquake hazard parameters from instrumental data for different regions in and around Turkey, *Eng. Geol.* **105**, 3-4, 200-210, DOI: 10.1016/j.enggeo.2009.02.004.
- Bozkurt, E. (2001), Neotectonics of Turkey – a synthesis, *Geodin. Acta* **14**, 1-3, 3-30, DOI: 10.1016/S0985-3111(01)01066-X.
- Bürgmann, R., M.E. Ayhan, E.J. Fielding, T.J. Wright, S. McClusky, B. Aktuğ, C. Demir, O. Lenk, and A. Türkezer (2002), Deformation during the 12 November 1999 Düzce, Turkey, earthquake, from GPS and InSAR data, *Bull. Seism. Soc. Am.* **92**, 1, 161-171, DOI: 10.1785/0120000834.
- Frohlich, C., and S.D. Davis (1993), Teleseismic  $b$  values; or, much ado about 1.0, *J. Geophys. Res.* **98**, B1, 631-644, DOI: 10.1029/92JB01891.
- Grassberger, P., and I. Procaccia (1983), Measuring the strangeness of strange attractors, *Physica* **9**, D, 189-208.

- Gutenberg, R., and C.F. Richter (1944), Frequency of earthquakes in California, *Bull. Seism. Soc. Am.* **34**, 185-188.
- Habermann, R.E. (1983), Teleseismic detection in the Aleutian Island arc, *J. Geophys. Res.* **88**, B6, 5056-5064, DOI: 10.1029/JB088iB06p05056.
- Huang, Q., A.O. Öncel, and G.A. Sobolev (2002), Precursory seismicity changes associated with the  $M_w=7.4$  1999 August 17 Izmit (Turkey) earthquake, *Geophys. J. Int.* **151**, 235-242, DOI: 10.1046/j.1365-246X.2002.01762.x.
- Kagan, Y.Y. (2007), Earthquake spatial distribution: the correlation dimension, *Geophys. J. Int.* **168**, 1175-1194, DOI: 10.1111/j.1365-246X.2006.03251.x.
- Kutoglu, H.S., and H. Akcin (2006), Determination of the 30-year creep trend on the Ismetpaşa segment of the North Anatolian Fault using an old geodetic network, *Earth Planets Space* **58**, 937-942.
- Kutoglu, H.S., H. Akcin, H. Kemaldero and K.S. Gormus (2008), Triggered creep rate on the Ismetpasa segment of the North Anatolian Fault, *Nat. Hazards Earth Syst. Sci.* **8**, 6, 1369-1373, DOI: 10.5194/nhess-8-1369-2008.
- Öncel, A.O., and T.H. Wilson (2002), Space-time correlations of seismotectonic parameters: examples from Japan and from Turkey preceding the İzmit earthquake, *Bull. Seism. Soc. Am.* **92**, 1, 339-349, DOI: 10.1785/0120000844.
- Özacar, A.A., C.B. Biryol, H. Tok, C.R. Gans, G. Zandt, S.L. Beck, L.M. Warren, and T. Taymaz (2009), *Passive Seismic Experiment for the North Anatolian Fault: Preliminary Reports*, 62nd Geological Kurultai of Turkey, 13-17 April 2009, MTA-Ankara, Turkey, p. 828.
- Öztürk, S. (2009), Deprem Tehlikesi ve Artçı Şok Olasılığı Değerlendirme Yöntemlerinin Türkiye'deki Depremlere Bir Uygulaması (An Application of the Earthquake Hazard and Aftershock Probability Evaluation Methods to Turkey Earthquakes), Ph.D. Thesis, Karadeniz Technical University, Trabzon, Turkey (in Turkish with English abstract), <http://tez2.yok.gov.tr>.
- Öztürk, S., Y. Bayrak, H. Çınar, G.Ch. Koravos, and T.M. Tsapanos (2008), A quantitative appraisal of earthquake hazard parameters computed from Gumbel I method for different regions in and around Turkey, *Nat. Hazards* **47**, 3, 471-495, DOI: 10.1007/s11069-008-9234-6.
- Polat, O., E. Gök, and D. Yılmaz (2008), Earthquake hazard of the Aegean extension region (West Turkey), *Turk. J. Earth Sci.* **17**, 3, 593-614.
- Reasenber, P. (1985), Second-order moment of central California seismicity, 1969-1982, *J. Geophys. Res.* **90**, B7, 5479-5495, DOI: 10.1029/JB090iB07p05479.
- Reilinger, R.E., S.C. McClusky, M.B. Oral, R.W. King, M.N. Toksöz, A.A. Barka, I. Kinik, O. Lenk, and I. Sanli (1997), Global Positioning System measurements of present-day crustal movements in the Arabia-Africa-Eurasia plate collision zone, *J. Geophys. Res.* **102**, B5, 9983-9999, DOI: 10.1029/96JB03736.

- Şaroğlu, F., Ö. Emre, and I. Kuşcu (1992), *Active Fault Map of Turkey*, General Directorate of Mineral Research and Exploration, Ankara, Turkey.
- Şengör, A.M.C., O. Tüysüz, C. İmren, M. Sakıncı, H. Eyidoğan, N. Görür, X.L. Pichon, and C. Rangin (2004), The North Anatolian Fault: A New Look, *Annu. Rev. Earth Planet. Sci.* **33**, 37-112.
- Toksöz, M.N., A.F. Shakal, and A.J. Michael (1979), Space-time migration of earthquakes along the North Anatolian Fault Zone and seismic gaps, *Pure Appl. Geophys.* **117**, 1258-1270.
- Turcotte, D.L. (1990), *Fractals and Chaos in Geology and Geophysics*, Cambridge University Press, Cambridge.
- Utsu, T. (1971), Aftershocks and earthquake statistics (III): Analyses of the distribution of earthquakes in magnitude, time and space with special consideration to clustering characteristics of earthquake occurrence (1), *J. Faculty Sci., Hokkaido University, Ser. VII (Geophys.)* **3**, 379-441.
- Wiemer, S. (2001), A software package to analyze seismicity: ZMAP, *Seismol. Res. Lett.* **72**, 2, 373-382.
- Wiemer, S., and K. Katsumata (1999), Spatial variability of seismicity parameters in aftershock zones, *J. Geophys. Res.* **104**, B6, 13135-13151, DOI: 10.1029/1999JB900032.
- Wiemer, S., and M. Wyss (1994), Seismic quiescence before the Landers (M=7.5) and Big Bear (M=6.5) 1992 earthquakes, *Bull. Seism. Soc. Am.* **84**, 3, 900-916.
- Wiemer, S., and M. Wyss (2000), Minimum magnitude of completeness in earthquake catalogs: Examples from Alaska, the Western United States, and Japan, *Bull. Seismol. Soc. Am.* **90**, 4, 859-869, DOI: 10.1785/0119990114.
- Yılmaz, V., M. Erişoğlu, and H.E. Çelik (2004), Probabilistic prediction of the next earthquake in the NAFZ (North Anatolian Fault Zone), Turkey, *Doğuş Üniversitesi Dergisi* **5**, 2, 243-250 (in English with Turkish abstract).

Received 7 January 2010

Received in revised form 19 August 2010

Accepted 25 October 2010